Absorption and emission spectroscopy of perylene ($C_{20}H_{12}$) isolated in Ne, Ar, and N_2 matrices

C. Joblin,[a] F. Salama, and L. Allamandola
NASA Ames Research Center, MS: 245-6, Moffett Field, California 94035

(Received 10 August 1998; accepted 19 January 1999)

The electronic absorption and emission spectra of perylene ($C_{20}H_{12}$) isolated in rare gas (Ne, Ar) and N_2 matrices are presented. While the electronic band systems show, in all matrices, the same fundamental frequencies as those observed in gas-phase jet experiments, the spectra in Ar and N_2 matrices exhibit much more spectral structure. The observed structure points to strong host–guest interactions and provides new insight into the low frequency modes of perylene. In particular, the spacing observed at 11 and 16 cm^{-1} in the S_0 and S_1 states, respectively, might be attributed to the gerade accordion mode of perylene. This mode, which has never been observed directly in jet experiments, could be induced into activity in solid matrices. © *1999 American Institute of Physics.* [S0021-9606(99)00915-0]

I. INTRODUCTION

Spectroscopic studies of isolated polycyclic aromatic hydrocarbons (PAHs) have become important in astrophysics since it was realized, over a decade ago, that these molecules may be an abundant component of the interstellar matter.[1] In particular, PAH molecular ions are considered to be plausible carriers for some of the diffuse interstellar bands (DIBs)[2] seen in the visible region of the spectrum. DIBs are absorption features that are produced by interstellar matter. Since their discovery in the early 1920s, these bands have challenged spectroscopists for most of this century. More than 100 DIBs have now been well observed in the whole visible to near IR spectral range[3] and the number of weaker features is expected to increase as deeper surveys become available.

Recent laboratory measurements support the proposal that some of the DIBs might arise from electronic transitions in PAH cations. Salama and Allamandola[4] have shown that most of the bands of the naphthalene cation ($C_{10}H_8^+$) fall at DIB positions, although they cannot account for the relative band intensities. At about the same time, a substituted pyrene cation was proposed to explain the strongest DIB, that at 4430 Å.[5] It has recently been shown that the carrier may be a photolysis product of methyl-pyrene, possibly the methylene-pyrene cation.[6] This cation appears to account for the 4430 and 7565 Å DIBs and possibly for two other weaker DIBs. Other promising DIB carriers include highly unsaturated hydrocarbon chains[7(a),7(b)] and the fullerene cation (C_{60}^+).[7(c)] A discussion of the various DIB carriers can be found in Ref. 8.

It has also been recognized that some of the DIBs have counterparts in emission, implying that the carriers of these bands should be free gas-phase molecular species.[9] To date, these optical emission bands have been observed in the Red Rectangle reflection nebula[9,10] and in the circumstellar envelope of the carbon rich star V854 Cent.[11] We have developed an experimental program to study the electronic luminescence of isolated PAH ions and thereby to test their relevance as potential carriers for the optical emission bands, and more generally for the DIBs. With the exception of the benzene cation and some of its derivatives[12(a),12(b)] and the

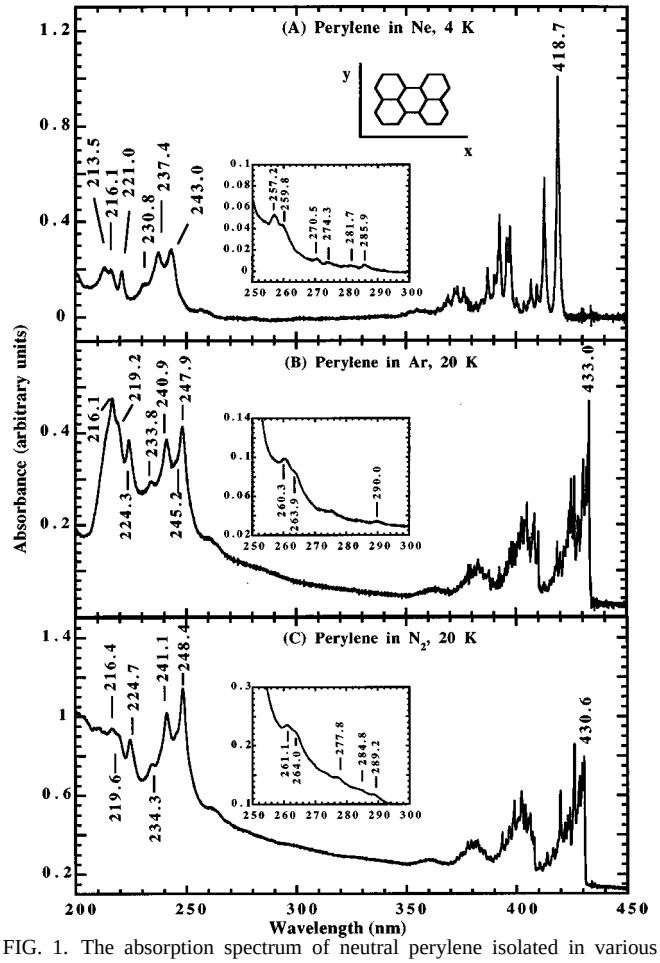

FIG. 1. The absorption spectrum of neutral perylene isolated in various matrices: (A) Ne at 4 K, (B) Ar at 20 K, and (C) N_2 at 20 K. The inserts display weaker bands which have been assigned to electronic transitions to states higher than the S_1 state of perylene (Table IV). These bands were measured for thicker deposits but their intensity has been scaled to the overall spectrum.

[a]Present address: CESR–CNRS, 9 Av. du Colonel Roche, 31028 Toulouse Cedex 04, France.

TABLE I. Band positions and associated vibrational spacings for the $S_1(B_{1u}) \leftarrow S_0(A_g)$ transition of neutral perylene isolated in Ne matrices at 4 K [Fig. 1(A) and Fig. 2(A)]. Two series of bands are observed which are referred to as site a and site b. Weaker bands are listed in parentheses.

Ne matrices				Jets[a]
λ (nm)	$\Delta\nu$ (cm^{-1})	λ (nm)	$\Delta\nu$ (cm^{-1})	$\Delta\nu$ (cm^{-1})
a		b		
418.7	0	419.4		
418.1 (sh)	34 (2×17?)			13?, 48
412.7	348	413.4	346	352
(412.1) (sh)	382 (348+34)			
(411.5) (sh)	418 (348+2×34)			426
409.4	543	410.0	547	548
406.8	699 (2×348)	407.6	690 (2×346)	704 (2×352)
(406.2) (sh)	735 (2×348+34)			
(405.5)	777 (429?+348)			776 (426+352)
(403.6)	894 (543+348)	(404.3)	891 (547+346)	897 (548+352)
(401.0)	1054 (3×348)			1054 (3×352)
(400.3)	1098	(401.0)	1094	1099
(399.8)	1129 (1098+34)			
397.2	1293	397.9 (sh)	1288	1293
395.6	1395	396.2 (sh)	1396	1398
392.4	1601	393.0 (sh)	1602	1603
391.8	1640 (1293+348)			
390.6	1718 (1369+348)			
390.2	1744 (1393+348)			
(388.9)	1830 (1293+543)			
387.1	1950 (1601+348)	(387.8) (sh)	1943 (1602+346)	
(384.9)	2097 (1395+2×348)	(385.5)	2097 (1396+2×346)	
(384.1)	2151 (1600+543)			
(383.6)	2185 (1293+543+348)			
(381.9)	2301 (1601+2×348)	(382.6)	2293 (1602+2×346)	
(380.5)	2398 (1293+1098)			
(379.0)	2502 (1601+543+348)			
(377.7)	2593 (2×1293)			
376.3	2691 (1395+1293)			
(374.9)	2790 (2×1395)			
373.4	2897 (1601+1293)	(374.1)	2887 (1602+1288)	
372.0	2998 (1601+1395)	(372.7)	2988 (1602+1396)	
(371.4) (sh)	3042 (1395+1293+348)			
(369.1)	3209 (2×1601)	(369.7)	3205 (2×1602)	
(368.6)	3246 (1601+1293+348)			
(367.2)	3350 (1601+1395+348)	(367.8)	3345 (1602+1396+346)	
(364.5)	3551 (2×1601+348)			
(354.9)	4293 (1601+1395+1293)			

[a]Values measured in jet experiments. From Refs. 19(a) and 19(b).

decacyclene anion,[12(c)] no studies of the luminescence of aromatic ions have been reported. In a previous short communication, we reported the preliminary evidence of fluorescence emission from the perylene cation ($C_{20}H_{12}^+$) isolated in inert gas matrices (Ne, Ar).[13] Evidence was found for medium-induced perturbations as well as site selectivity. In the course of this work we have carried out an extensive study of neutral perylene absorption and emission in neon, argon, and nitrogen matrices. Here we report the results. In a forthcoming paper, we will discuss the detailed spectroscopy of the perylene cation.

II. EXPERIMENT

The experimental setup, a cryogenically cooled vacuum chamber, equipped with a UV–visible–near IR spectrograph, has been described in detail in Ref. 14. After passing through the sample, the light is collected through an optical fiber cable and is guided to the entrance slit of a 0.5 m monochromator (Acton Research Corporation). The detector is a 298 ×1152 pixels charge-coupled device (CCD) area array (Princeton Instruments) thermoelectrically cooled to −40 °C. Only the longest axis of the CCD detector is used for spectroscopy measurements while pixels are binned along the shorter axis to increase the signal-to-noise ratio. Absorption spectra are measured with a deuterium lamp in the UV, from 200 to 450 nm, and a quartz tungsten halogen lamp in the visible and near IR from 360 to 2500 nm. For emission measurements, the excitation source and the detection system light paths are at 90° with respect to one another, and the sample window is positioned at about 30° with respect to the excitation source axis (in order to minimize direct reflected light on the detector). The quartz tungsten halogen lamp is

TABLE II. Band positions and associated vibrational spacings for the $S_1(B_{1u}) \leftarrow S_0(A_g)$ transition of neutral perylene isolated in Ar matrices at 20 K [Figs. 1(B) and Fig. 2(B3)]. Five main origins have been observed and associated with different sites a to e. The assignment of the origin of sites a and b is questionable. A second possibility listed with bold values is discussed in the text (Sec. III C). Weaker bands are listed in parentheses.

Ar matrices				Jets[a]
λ (nm)	$\Delta\nu$ (cm^{-1})	λ (nm)	$\Delta\nu$ (cm^{-1})	$\Delta\nu$ (cm^{-1})
a		b		
433.0	0 (−**11**)	431.8	0 (−**11**)	
432.8 (sh)	11? (**0**)	431.6 (sh) ?	(**0**?)	
432.5	27 (**16**)	431.3	27 (**16**)	13?,48
		431.0	43 (27+16?) (**2×16**)	
426.4	357	425.3	354[b]	352
425.9	385 (357+27)			
425.3	418[b]			426
424.8	446 (418+27)			
422.9	551			548
(422.5)	574 (551+27)			
420.0	715 (2×357)	(418.9)	713 (2×354)	704 (2×352)
419.6	738 (715+27)			
418.5	800 (418+357+27)			
(416.6)	909 (551+357)			897 (548+352)
(413.9)	1066 (3×357)			1054 (3×352)
(413.3)	1101 (2×551)	412.4	1089[b]	1099
412.4	1154[b]			
410.0	1296	408.9	1297	1293
409.5	1325 (1296+27)			
408.1	1409	407.2	1399	1398
404.7	1615	403.7	1612[b]	1603
402.2	1769[b] (1409+357)	(401.2)	1766 (1399+354)	
(400.8)	1855[b] (1296+551)			
(398.9)	1974 (1615+357)	398.0	1967[b] (1612+354)	
(398.5) (sh)	1999[b] (1615+357+27)			
		(395.7)	2113 (1399+2×354)	
(395.9)	2164 (1615+551)			
(395.2)	2209 (1296+551+357)			
(393.3)	2331 (1615+2×357)			
(392.0)	2416 (1615+418+357+27)			
(387.5)	2712 (1409+1296)			
(387.2)	2732 (1409+1296+27)			
c		e		
430.3	0	428.0	0	
430.0 (sh)	16	427.7 (sh)	16	13?, 48
429.7 (sh)	32 (2×16)	427.4 (sh)	32 (2×16)	
		427.1 (sh)	49 (3×16)	
423.9	351	421.6	355	352
423.6 (sh)	368 (351+16)	421.3 (sh)	371 (355+16)	
(423.3) (sh)	384 (351+2×16)	(421.0) (sh)	388 (355+2×16)	
		(418.1)	553	548
		417.6	582[b] (553+2×16)	
		417.3 (sh)	599[b] (553+3×16)	
417.7	701[b] (2×351)			704 (2×352)
417.3	724[b] (701+16)	415.1	726 (2×355+16)	
		(414.9) (sh)	738 (2×355+2×16)	
(414.3)	897 (546?+351)			897 (548+352)
		(408.7) (sh)	1103	1099
407.7	1288	405.8	1278[b]	1293
		405.5 (sh)	1296[b] (1278+16)	
405.8	1403[b]	403.7	1406[b]	1398
405.4 (sh)	1427[b] (1403+16)			
402.5	1605	400.2	1623 (1607+16)	1603
402.2	1624[b] (1605+16)			
401.8 (sh)	1648 (1605+2×16)			
400.0	1760 (1403+351)	398.0	1761[b] (1406+355)	
399.7	1779 (1760+16)	397.7	1780 (1761+16)	
396.8	1962 (1605+351)			
396.5 (sh)	1981 (1605+351+2×16)			

TABLE II. (*Continued*.)

Ar matrices				Jets[a]
λ (nm)	$\Delta\nu$ (cm^{-1})	λ (nm)	$\Delta\nu$ (cm^{-1})	$\Delta\nu$ (cm^{-1})
d				
428.4	0			
428.1	16			
422.0	354			352
418.5	552[b]			548
405.8	1300[b]			1293
404.2	1398			1398
400.8	1607[b]			1603
398.5 (sh)	1751[b] (1404+354)			

[a]Values measured in jet experiments. From Refs. 19(a) and 19(b).
[b]Bands with several possible assignments.

also used as the excitation source. Radiation from the lamp is filtered with a 0.2 m monochromator (Photon Technology Instrument) to provide broadband excitation [typically 20 nm full width at half-maximum (FWHM) and 40 nm base width for slit aperture of 6 mm]. The spectrograph entrance slit is 30 μm for absorption measurements and 300 μm for the emission measurements of neutrals. The spectral resolution is less than 0.1 nm and about 0.5 nm for the absorption and emission spectra respectively. Wavelength calibration is achieved using discharge calibration lamps. The band positions given in this study are averaged over several experiments.

Neon (argon or nitrogen) gas and perylene, evaporated under vacuum from an oven ($T\sim 115\,^{\circ}C$), are codeposited on the cold (4.2–20 K) sapphire window of a continuous flow liquid helium cryostat. The matrix gas to perylene ratio is estimated to be about 1000. In a typical experiment, a first layer is deposited during about 60 min. The absorption spectrum of neutral perylene is recorded after 10 min. deposit and at the end of the deposit to monitor the growth and the quality of the matrix. The fluorescence spectrum is generally measured after the total deposit.

III. RESULTS AND DISCUSSION

A. Absorption

The absorption spectra of neutral perylene isolated in Ne, Ar, and N_2 matrices are shown in Figs. 1(A), 1(B), and 1(C), respectively. The bands and associated vibrational spacings for the $S_1(B_{1u})\leftarrow S_0(A_g)$ transition are reported in Tables I–III. Transitions to higher electronic excited states are listed in Table IV where a tentative assignment is proposed following the work of Tanizaki *et al.*[15(a)] Some of the transitions were previously reported in Ar matrices from fluorescence excitation spectra.[15(b)] The inserts in Fig. 1 display weak bands which have been assigned to neutral perylene states higher than S_1. These bands are better observed after long deposits for which the $S_1\leftarrow S_0$ system is saturated.

The $S_1\leftarrow S_0$ transition of perylene in Ar and N_2 matrices exhibits much more structure than does the same transition observed in Ne matrices. The bands are listed in Tables II and III for a 20 K deposit. We note that considerable spectral congestion is observed for a more amorphous 4 K Ar matrix [Fig. 2(B1)]. The strong temperature dependence of the structure indicates that it arises from multiple site formation in the solid matrix. This temperature-dependent effect is often observed in matrices when a large number of different sites is formed.[16] Amongst the complex structure observed in Ar and N_2, different sites in the solid matrix named a to e in Ar and a to d in N_2 have been identified. Other substructures have been assigned to low frequency spacings whose possible origin is discussed in Sec. III C.

The absorption spectrum of neutral perylene in Ar and Ne matrices has been partly reported in the literature[15(b),17,18] but has never been discussed in detail. As illustrated in Fig. 2(A), in Ne matrices, each band of the $S_1(B_{1u})\leftarrow S_0(A_g)$ system is composed of a sharp component showing weaker substructure [a in Table I and Fig. 2(A)] as well as a broader and slightly redshifted band (b). A similar profile was obtained by Tamm and Saari in Ne.[18] Table I lists the two series of bands associated with species a and b whose transition origins fall at 418.7 and 419.4 nm, respectively. These values can be compared with the value of 415.5 nm in jet experiments.[19(a)–19(c)] The vibrational spacings which are reported for a and b in Table I are very close to the spacings observed in the jet experiments[19(a),19(b)] Therefore, we assign species a and b to the isolated perylene molecule trapped in two different sites in Ne matrices.

As shown in Figs. 2(B1), (B2), and (B3), the origin of the $S_1\leftarrow S_0$ transition of neutral perylene in Ar matrices can be broken into many band systems whose origins fall at 433.0, 431.8, 430.3, 428.4, and 428.0 nm, respectively, for a 20 K deposit [Fig. 2(B3)]. This corresponds to blueshifts of 64, 145, 248, and 270 cm^{-1} relative to the 433.0 nm band. All the band systems and the associated substructures are listed in Table II. The vibrational spacings which are derived are close to those measured in jet experiments.[19(a),19(b)] Regular low-frequency spacings have also been derived from the spectra and listed in Tables I–III. Their assignment, which is not unique particularly in the case of sites a and b in Ar matrices (Table II), will be discussed in Sec. III C.

The spectrum and behavior of perylene in N_2 matrices

TABLE III. Band positions and associated vibrational spacings for the $S_1(B_{1u})\leftarrow S_0(A_g)$ transition of neutral perylene isolated in N_2 matrices at 20 K [Fig. 1(C), 2(C1), and 2(C2)]. Four main origins have been observed and associated with sites a–d. Weaker bands are listed in parentheses.

N_2 matrices				Jets[a]
λ (nm)	$\Delta\nu$ (cm^{-1})	λ (nm)	$\Delta\nu$ (cm^{-1})	$\Delta\nu$ (cm^{-1})
a		b		
430.6	0	429.6	0	
430.3	16	429.3 (sh)	16	13?, 48
430.0	32 (2×16)			
424.1	356	423.2	352	352
(423.7) (sh)	378 (356+16)	(422.7) (sh)	380 (352+2×16)	
420.7	546			548
417.8	711 (2×356)			704 (2×352)
407.9	1292	407.1	1287	1293
(407.6) (sh)	1310 (1292+16)	(406.6) (sh)	1317 (1287+2×16)	
406.1	1401	405.3	1396	1398
405.8 (sh)	1419[b] (1401+16)			
402.8	1603	402.0	1598[b]	1603
402.3	1634[b] (1603+2×16)			
(400.4)	1752 (1401+356)			
399.0	1839[b] (1292+546)			
398.7 (sh)	1858 (1839+16)			
397.1	1959 (1603+356)			
(385.8)	2697 (1401+1292)	(385.2)	2683 (1396+1287)	
(381.4)	2996 (1603+1401)			
(376.0)	3372[b] (1603+1401+356)			
c		d		
428.4	0	426.2	0	
428.1 (sh)	16			13?, 48
		425.6 (sh)	33 (2×16)	
(427.6)	44 (3×16)	425.2 (sh)	55 (3×16)	
(427.2)	66 (4×16)			
421.9	360 (344+16)	419.9	352	352
421.6 (sh)	376 (344+2×16)	419.3 (sh)	386 (352+2×16)	
		418.7	420	426
		416.5	546	548
		(416.3) (sh)	558 (546+16)	
415.9 (sh)	702 (2×344+16)	413.8	703 (2×352)	704 (2×352)
(412.5)	900 (556+344)	(410.5)	897 (546+352)	897 (548+352)
405.8	1300[b]	404.0	1289[b]	1293
		403.7 (sh)	1308 (1289+16)	
404.3 (sh)	1391	402.3	1394[b]	1398
		402.0	1412[b] (1394+16)	
(400.9)	1601	399.0	1599[b]	1603
398.4	1758 (1391+344+16)	396.7	1745 (1394+352)	
(398.0) (sh)	1783 (1391+344+3×16)			
(395.3)	1955 (1601+344+16)	393.5	1950 (1599+352)	
(383.9)	2706 (1391+1300+16)	(382.4)	2687 (1394+1289)	
(382.8)	2781 (2×1391)			
(381.0)	2904 (1601+1300)			
(379.4)	3015 (1601+1410)	(377.9)	2999 (1599+1394)	
		(377.2)	3048 (1394+1289+352+16)	
(376.0)	3253[b] (1601+1300+360)			
		(375.0)	3203 (2×1599)	
		(374.4)	3246[b] (1599+1289+352)	
(374.4)	3367[b] (1601+1410+360)	(373.0)	3346 (1599+1394+352)	

[a]Values measured in jet experiments. From Refs. 19(a) and 19(b).
[b]Bands with several possible assignments.

are comparable to those observed in Ar matrices: for a 4 K deposit, the spectrum exhibits spectral congestion whereas four main band systems falling at 430.6, 429.6, 428.4, and 426.2 nm, respectively, dominate the spectrum for a 20 K deposit [Fig. 2(C)]. Blueshifts of 54, 119, and 240 cm^{-1} relative to the 430.6 nm band are measured. The vibrational spacings which are derived are close to those measured in jet experiments. According to the approach adopted in the cases of Ar and Ne matrices, a low-frequency spacing of 16 cm^{-1} has been introduced to account for the spectral complexity.

TABLE IV. Absorption bands of neutral perylene in Ne and Ar matrices involving electronic states at higher energy than the S_1 state (cf. Fig. 1). Weaker bands are listed in parentheses. A tentative assignment is made using the work of Tanizaki *et al.* [Ref. 15(a)] and the perylene configuration represented in Fig. 1.

$C_{20}H_{12}$/Ne		$C_{20}H_{12}$/Ar		$C_{20}H_{12}$/N_2		PVA film[a]	Calc.[a]	Sym[a]
λ (nm)	$\Delta\nu$ (cm^{-1})	λ (nm)	$\Delta\nu$ (cm^{-1})	λ (nm)	$\Delta\nu$ (cm^{-1})	λ (nm)	λ (nm)	
(285.9)	0	(290.0)	0	(289.2)	0		289	A_g ?
(281.7)	521			(284.8)	534		276	A_g ?
(274.3)	1479			(277.8)	1419			
(270.5)	1991 (1479+521)							
(259.8)	0	(263.9)	0	(264.0)	0		261	B_{2g}
(257.2)	389	(260.3)	524	(261.1)	421			
243.0	0	247.9	0	248.4	0	266	250	B_{3u}
		245.2	444	245.3	509			
237.4	0	240.9	0	241.1	0	256	240	B_{1u}
230.8	1204	233.8	1260	234.3	1204		233	A_g ?
221.0	0	224.3	0	224.7	0	230	212	B_{1u}
216.1	1026	219.2	1037	219.6	1013		211	B_{3u}
213.5	0	216.1	0	216.4	0	220	207	B_{1u}

[a]Reference 15(a).

B. Fluorescence

Strong blue emission is observed upon electronic excitation of matrix isolated neutral perylene at about 400 nm. The fluorescence yield of neutral perylene is very high (~0.9) according to measurements in solution,[20] and in jets of gas-phase molecules.[21] The phosphorescence emission is expected to be very weak.[20(b)] It was measured at about 794 nm in solution[20(c)] but was not detected in our experiment.

Figures 3 and 4 compare the fluorescence and absorption spectra of perylene isolated in Ne and Ar matrices. The emission spectrum mirrors the multicomponent structure observed in the absorption spectrum (Tables I, V, and II, VI). Low-frequency spacings were introduced to account for the structure observed in Ar matrices. The emission spectra displayed in Figs. 3 and 4 were pumped with an excitation band of 20 nm FWHM centered at 400 nm. No changes were observed in the band positions, profiles, and relative intensities of the fluorescence spectra when tuning the central excitation wavelength from 395 to 412 nm. This indicates that the observed fluorescence is vibrationally relaxed. In addition, except for the shift induced by the matrix, the fluorescence spectrum of perylene in neon is very similar to the fluorescence spectrum measured in jets by exciting the origin of the S_1 state.[19(c)] The vibrational spacings which are derived are therefore very close to those measured in jet experiments (Tables V and VI). They are also consistent with the fundamental vibrations of the S_0 state of perylene measured by IR[17] and Raman[22] spectroscopy (Table VII).

C. Discussion

The spectra presented in this paper are typical of the results obtained in many experiments. Spectral reproducibility gives us confidence in the reported band structures. The spectrum of perylene is very sensitive to the solid matrix environment. This interaction with the matrix does not significantly affect the perylene vibrational frequencies which are close to those observed in the gas phase, but can lead to very complex substructures.

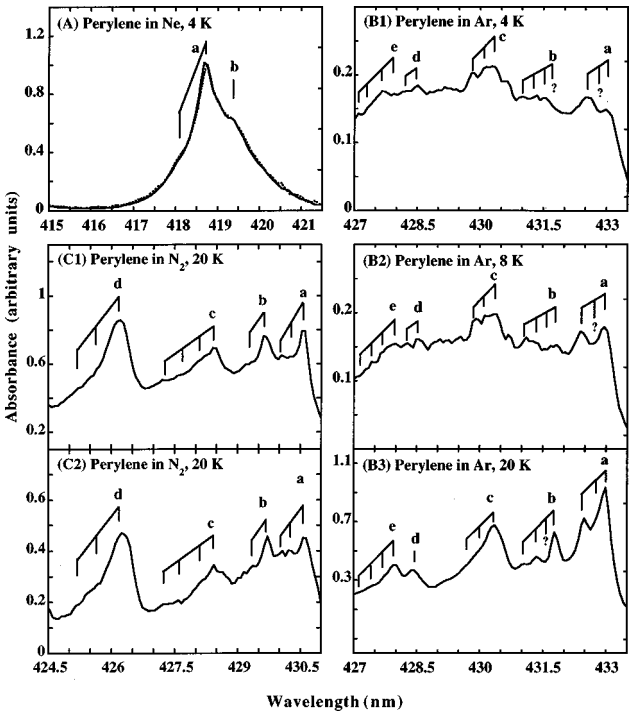

FIG. 2. The origin of the $S_1(B_{1u}) \leftarrow S_0(A_g)$ absorption spectrum of neutral perylene in (A) Ne matrices, in (B1), (B2), and (B3) Ar matrices, and in (C1) and (C2) N_2 matrices. In 4 K Ne matrices, the spectrum is very similar from one experiment to the other as shown by the plain and dotted lines in (A). In Ar matrices, the spectrum is very sensitive to the matrix temperature as illustrated in (B1), (B2), and (B3). Using as a guideline the 20 K spectrum, the observed structure has been split in different sites (a–e) and associated substructures (indicated by connected vertical ticks) which are likely to be due to a low-frequency mode of perylene (cf. Sec. III C). The reproductibility of the spectrum with temperature is illustrated by (C1) and (C2): two experiments performed in N_2 matrices at 20 K.

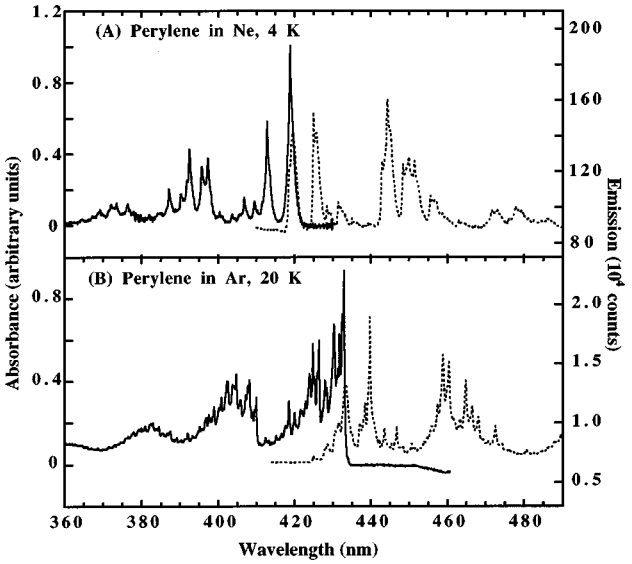

FIG. 3. The entire $S_1(B_{1u}) \leftarrow S_0(A_g)$ absorption spectrum (the continuous line) and the fluorescence spectrum (the dotted line) of neutral perylene isolated in (A) a Ne matrix at 4 K and in (B) an Ar matrix at 20 K. The fluorescence emission is induced by broadband excitation centered at 400 nm and with 20 nm FWHM.

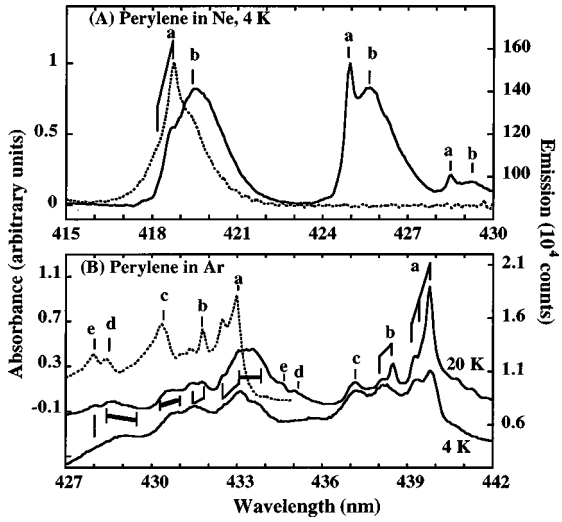

FIG. 4. The origin of the $S_1(B_{1u}) \leftarrow S_0(A_g)$ absorption spectrum (the dotted line) and of the fluorescence emission (the continuous line) of neutral perylene isolated in (A) a Ne matrix at 4 K and in (B) an Ar matrix at 20 K. The fluorescence spectrum in Ar matrices at 4 K is also shown [the lower spectrum in (B)]. The fluorescence was induced by broadband excitation centered at 400 nm and with 20 nm FWHM. The letters point to the different sites which are listed in Tables I, II and V, VI and further discussed in the text. The connected vertical ticks underline the presence of low-frequency spacings which are likely to be associated to a low-frequency mode of perylene (cf. Sec. III C). Thin and thick connecting lines show the evidence for the low-frequency mode in the S_1 and S_0 states, respectively.

In Ne matrices, the absorption spectrum exhibits two series of bands designated as species a and b whose origins fall at 418.7 ($23\,883\,\mathrm{cm}^{-1}$) and 419.4 nm ($23\,844\,\mathrm{cm}^{-1}$), respectively (Table I). In gas-phase jet experiments, the origin falls at 415.5 nm ($24\,067 \pm 2\,\mathrm{cm}^{-1}$).[19(a)–19(c)] The gas-phase to matrix relative shift ($\Delta\nu/\nu_{\mathrm{gas}}$) is 0.76% and 0.93% for a and b, respectively. This is to compare to the 0.25% value measured for the smaller molecule, naphthalene, in a neon matrix.[4(a)] The vibrational spacings which are reported for a and b, in Table I are also very close to the spacings observed in jet experiments.[19(a)] A simple explanation is therefore to identify species a and b with perylene trapped in two different sites formed in Ne matrices. The increase in the redshift observed when going from naphthalene to perylene translates to the increasing interaction of the guest molecule with the host as the molecular size increases. Also, the increasing shift when going from site a to site b indicates that the perylene molecule is more perturbed in the latter site. These observations seem to agree with the conclusions of MacDonald *et al.*[16] that substitutional sites for PAHs in inert matrices are formed by displacement of six or more inert gas atoms.

The origin of the $S_1 \leftarrow S_0$ transition of neutral perylene in Ar matrices is considerably more complex, especially for a 4 K deposit where spectral congestion is observed (Fig. 2). The warming-up of the matrix (up to about 35 K) leads to an increase of the intensity of the bands associated with species a relative to the others. This behavior tends to indicate that sites of type a are dominantly formed in the matrix upon rearrangement of its solid structure. All of the substructure observed in Ar matrices could be explained by a large number of sites. However, regular spacings can be seen in the observed substructure with averaged values of $16\,\mathrm{cm}^{-1}$ for sites c and e, and $27\,\mathrm{cm}^{-1}$ (and possibly $11\,\mathrm{cm}^{-1}$) for sites a and b. Furthermore, the absorption bands associated with sites c and e in 20 K matrices exhibit extended blue wings which are difficult to explain by site effects. The $16\,\mathrm{cm}^{-1}$ spacing is also clear in absorption in N_2 matrices and marginally observed in Ne matrices. These results suggest that the $16\,\mathrm{cm}^{-1}$ spacing is the fundamental frequency of a low-frequency mode in the S_1 state of perylene. Looking at Fig. 2(B1), 2(B2), and 2(B3), it appears that the intensity of the different bands associated with each site varies with temperature. This suggests that the intensity variation is induced by the formation of additional sites in the 4 K matrices.

The fundamental frequency of the low-frequency mode in the S_0 state is more difficult to determine. The assignment of substructures in the fluorescence spectra in Ar matrices suggests a fundamental frequency of $11\,\mathrm{cm}^{-1}$ in the S_0 state (Table VI). Note, however, that the measured spacings are smaller than the expected resolution for fluorescence measurements ($\sim 20\,\mathrm{cm}^{-1}$) and thus might be questionable. This value of $11\,\mathrm{cm}^{-1}$ is compatible with a new assignment of the substructure observed in absorption in Ar matrices for sites a and b. The first assignment made in Tables II and VI involves a spacing of $27\,\mathrm{cm}^{-1}$, which is not observed for the other sites nor for the other matrices. The new assignment (the bold values in Tables II and VI) reveals spacings of 16 and $11\,\mathrm{cm}^{-1}$ in the S_1 and S_0 states, respectively, similar to those derived for the other Ar sites as well as observed in Ne and N_2 matrices. This assignment implies that the low-frequency mode is radiatively populated in the S_0 and S_1 states for sites a and b in Ar matrices, and therefore that the coupling with the matrix phonons depends both on the nature of the matrix as well as on the site structure.

The lowest frequency mode of perylene is the gerade

TABLE V. Band positions and associated vibrational spacings for the fluorescence of neutral perylene isolated in Ne matrices at 4 K [Figs. 3(A) and 4(A)]. The two sites a and b which are observed in absorption (Table I) are also seen in emission. Weaker bands are listed in parentheses.

Ne matrices				Ne[a]/Jets[b]
λ (nm)	$\Delta\nu$ (cm^{-1})	λ (nm)	$\Delta\nu$ (cm^{-1})	$\Delta\nu$ (cm^{-1})
a		b		
418.7	0	419.4	0	
425.0	354	425.7	353	360/353
426.3 (sh)	427			427
428.5	546	429.2	544	550/547
431.5	708 (2×354)	432.2	706 (2×353)	
433.0 (sh)	789	(433.8) (sh)	791	790/
435.1	900 (546+354)	(435.8)	897 (544+353)	
(436.6)	979 (546+427)			
(438.2)	1063 (3×354)	(439.0)	1065 (3×353)	
		(439.9)	1106	1100/1102
		(440.7)	1152 (791+353)	
442.9	1304	443.7	1291	–/1300
444.3	1376	445.0	1372	1380/1373
448.4	1581	449.3	1587	1580/1580
449.9	1656 (1304+354)			
451.4	1730 (1376+354)	452.2 (sh)	1729 (1372+353)	
455.6	1934 (1581+354)	456.5	1938 (1587+353)	
457.2	2011 (1304+2×354)			
(458.7)	2082 (1376+2×354)			
(459.6)	2125 (1581+546)			
(463.0)	2285 (1581+2×354)	(463.9)	2287 (1587+2×353)	
(464.6)	2360 (1304+3×354)			
(470.1)	2611 (2×1304)			
471.6	2679 (1376+1304)	472.3	2671 (1372+1291)	
473.2	2751 (2×1376)	(474.0) (sh)	2746 (2×1372)	
(476.2)	2884 (1581+1304)	(476.9) (sh)	2875 (1587+291)	
(477.7)	2949 (1581+1376)	(478.7) (sh)	2954 (1587+1372)	
(479.5)	3028 (1376+1304+354)	(480.2) (sh)	3019 (1372+1291+353)	
(481.1)	3098 (2×1376+354)			
(482.6)	3162 (2×1581)			
(484.3)	3235 (1581+1304+354)			
(486.0)	3307 (1581+1376+354)	(487.0) (sh)	3310 (1587+1372+353)	
(487.8) (sh)	3383 (1581+1376+427)			
(491.1)	3521 (2×1581+354)			
(492.8)	3591 (2×1581+427)			
(494.5)	3661 (1581+1376+2×354)			
(504.4)	4058 (2×1376+1304)			
(509.8)	4268 (1581+1376+1304)			
(511.3)	4325 (1581+2×1376)			
(516.7)	4530 (2×1581+1376)			
(518.5)	4597 (1581+1376+1304+354)			
(520.6)	4675 (1581+2×1376+354)			

[a]Values measured in Ne matrices. From Ref. 18.
[b]Values measured in jet experiments. From Refs. 19(a) and 19(b).

accordion mode.[23,19(b)] Indirect estimation in jet experiments led to the values of 20 and 13 cm^{-1} for this mode in the ground (S_0) and excited (S_1) states, respectively.[19(b)] The gerade accordion mode can be described as the *trans*-out-of plane bending of the two naphthalene moieties on each side of a plane containing the central cycle of perylene. The accordion mode is symmetry forbidden in the free molecule[23] but might be induced into activity in the perturbing environment of solid matrices. Furthermore, this mode being very close to the lattice's phonon modes, strong coupling between the host molecule and the matrix is expected. The difference in the one-phonon density of state distribution between the various matrices[24] could therefore account for the observed spectral diversity and complexity from one matrix to the other. For instance, the phonon density at 11 and 16 cm^{-1} is higher in Ne matrices than in Ar matrices. A faster relaxation of the low-frequency mode is therefore expected in Ne matrices compared to Ar matrices, which is consistent with the fact that hot bands involving this mode (bands at -11 and -16 cm^{-1} in Tables II and VI, respectively) are observed in Ar and not in Ne matrices. A faster relaxation is also expected in 20 K Ar matrices relative to 4 K matrices because of increased phonon density at higher temperature. We note that the *direct* measurement of the accordion mode in solid matrices leads to values which are close to the values indirectly determined in jet experiments. However, the funda-

TABLE VI. Band positions and associated vibrational spacings for the fluorescence of neutral perylene isolated in Ar matrices at 20 K [Figs. 3(B) and 4(B)]. The various species a–e which are observed in absorption (Table II) are also prominent in the fluorescence spectrum. The bold values for sites a and b show a different assignment for the band origin (see discussion in Sec. III C). Weaker bands are listed in parentheses.

Ar matrices				Jets[a]
λ (nm)	$\Delta\nu$ (cm^{-1})	λ (nm)	$\Delta\nu$ (cm^{-1})	$\Delta\nu$ (cm^{-1})
		a		
432.5	−27 (**-16**)			
432.8 (sh)?	−11 (**0**)			
433.0	0 (**11**)			
433.6	32 (3×11) (**4×11**)			
439.2	326 (352−27)			
439.5 (sh)	342 (352−11)			
439.7	352			353
440.8	409[b] (434−27)			
441.3	434[b]			427
443.0	521 (547−27)			
443.3 (sh)	537 (547−11)			
443.5	547			547
446.2	683 (713−27)			
446.5 (sh)	698 (713−11)			
446.8	713 (2×352)			
458.3 (sh)	1275 (1303−27)			
458.9	1303[b]			1300
459.8	1346 (1374−27)			1373
460.4	1374			
464.2 (sh)	1552 (1580−27)			
464.8	1580			1580
465.9 (sh)	1631 (1658−27)	500.0	3095 (2×1374+352)	
466.5	1658[b] (1303+352)	501.5	3155 (2×1580)	
(467.6)	1709 (1732−27)	503.4	3230 (1580+1303+352)	
468.1	1732 (1374+352)	(504.5) (sh)	3273 (3304−27)	
471.9	1904 (1935−27)	505.3	3304 (1580+1374+352)	
472.6	1935 (1580+352)	(510.8)	3518 (2×1580+352)	
(473.7)	1984 (2011−27)	(512.6)	3586 (1580+1303+2×352)	
(474.3)	2011 (1303+2×352)	(514.7)	3666 (1580+1373+2×352)	
(476.1)	2091 (2130−27)	(520.1)	3868 (2×1580+2×352)	
(477.0)	2130 (1580+547)	(521.1)	3905 (3×1303)	
480.7	2292 (1580+2×352)	(523.0)	3974 (1374+2×1303)	
(485.2)	2485 (1580+547+352)	(525.1)	4051 (2×1374+1303)	
488.0	2603 (2×1303)	(528.6)	4177 (1580+2×1303−11?)	
489.7	2674 (1374+1303)	(529.8) (sh)	4220 (4252−27)	
491.0 (sh)	2728 (2753−27)	(530.7)	4252 (1580+1374+1303)	
491.6	2753 (2×1374)	(532.6)	4319 (1580+2×1374−11?)	
494.6	2876 (1580+1303)	(536.3)	4448 (2×1580+1303−11?)	
495.7 (sh)	2921 (2950−27)	(538.5)	4525 (2×1580+1374−11?)	
496.4	2950[b] (1580+1374)	(540.7)	4600 (1580+1374+1303+352−11?)	
498.3	3026 (1374+1303+352)	(542.8)	4672 (1580+2×1374+352−11?)	
b		c		
431.3	−27 (−16)			
431.6 (sh)	−11 (**0**)	430.3 (sh)	0	
431.8	0 (**11**)	430.5	−11	
		436.9 (sh)	351	353
438.5	354	437.1	361 (351+11)	
(441.8)	524 (545−27)			
442.2	545	440.8	554[b]	547
445.4	707 (2×354)	(444.0)	722 (2×351+2×11)	
		(444.5)	742 (2×351+4×11)	
		(450.7)	1052 (3×351)	
		(451.3)	1081 (3×351+3×11)	
		455.5 (sh)	1286 (1300−16)	
457.5	1301[b]	456.0	1310 (1300+11)	1300
458.9	1368[b]	457.5	1382[b]	1373
(463.0)	1561 (1575−11)	(461.7)	1581	
463.3	1575	(462.0) (sh)	1595 (1581+11)	1580
466.5	1723[b] (1368+354)			
(470.7)	1914 (1575+354−11)	(469.3)	1931 (1581+351)	
(471.0)	1927 (1575+354)			

TABLE VI. (*Continued*.)

Ar matrices				Jets[a]
λ (nm)	$\Delta\nu$ (cm^{-1})	λ (nm)	$\Delta\nu$ (cm^{-1})	$\Delta\nu$ (cm^{-1})
		(477.0)	2275 (1581+2×351)	
(486.3)	2595 (2×1301)			
		(492.9)	2951 (1581+1382)	
496.4	3014[b] (1368+1301+354−11)			
d		e		
428.4	0	428.0	0	
(435.0)	354	434.6	355	353
		438.1	539	547
		441.3	704[b] (2×355)	
		(445.0)	893 (539+355)	
		(448.4)	1063 (3×355)	
		(454.8)	1377	1373

[a]Values measured in jet experiments. From Refs. 19(a) and 19(b).
[b]Bands with several possible assignments.

mental frequency is measured to be higher in the excited state than in the ground state which differs from the previous measurements in jets by Fourmann *et al.*[19(b)] Unfortunately, it is not clear how the authors have extracted their values from the gas-phase spectra. A further comparison of the frequencies measured in jets and in matrices is therefore not possible at this stage.

TABLE VII. Fundamental frequencies of the S_0 state of perylene derived from fluorescence measurements in rare gas matrices (several sites) compared to those measured by IR and Raman spectroscopy.

Fluorescence (*this work*)		IR[a]	Raman (A_g)[b]
Ne matrices ν (cm^{-1})	Ar matrices ν (cm^{-1})	Ar matrices ν (cm^{-1})	Crystalline phase ν (cm^{-1})
11			73, 62, 43, 35
			176
			297[c]
354, 353	352, 354, 351, 354, 355		364[c]
427	434		
546, 544	547, 545, 544, 539		548[c]
		772, 765	
789, 791		791.2	784[c]
		815.4, 810.9	844
		969.5	979[c]
		1046.7	1045
1106		1089, 1088.2	1103[c]
		1132, 1130.8	1140[c]
		1156	
		1187, 1188	
		1218, 1216	1222
		1280.4	1291
1304, 1291	1303, 1301, 1300	1288.6	1299[c], 1295
		1334.8	
1376, 1372	1374, 1368, 1382, 1377	1374.5	1373[c], 1367[c]
		1385.1	
		1399, 1396.2	
		1494.2	
		1500.5	
1581, 1587	1580, 1575, 1581	1597.4	1579, 1568[c]
		1613.5	1620
		3057	
		3065	
		3069	
3098	3095	3095	

[a]From Ref. 17.
[b]From Ref. 22.
[c]Vibrations with A_g symmetry.

Several studies on complexes of perylene with argon have shown that the origin position depends on the degree of complexation, as well as on the presence of intermolecular low-frequency modes and their role in the energy relaxation.[25(a)–25(d)] In particular, Wittmeyer and Topp[25(c)] have reported a resonance at 16 cm^{-1} in the absorption spectrum of perylene–Ar_n complexes containing argon trimers. This resonance was attributed to Ar–Ar motion. Interestingly enough, in our experiments, the 16 cm^{-1} spacing was observed in Ar, N_2, and Ne matrices and attributed to a low-frequency mode of perylene (possibly the gerade accordion mode). We suggest that this mode, which is symmetry forbidden for the isolated molecule, becomes active both in solid matrices and in clusters.

IV. CONCLUSION

This paper presents the electronic absorption and emission spectra of matrix isolated perylene. The perylene spectra in Ar and N_2 are more complex than that in Ne. While the principal features in all matrices show the same fundamental frequencies as in gas-phase jet experiments, the behavior in Ar and N_2 reveals multiple site formation and the possible signature of a low-frequency mode of perylene, most probably the accordion mode which is induced into activity in the matrix environment. The fundamental frequency measured for this mode in Ne, Ar, and N_2 matrices is 16 cm^{-1} in the S_1 state. A value of 11 cm^{-1} for the S_0 state was deduced from the measurements in Ar matrices.

Complementary experiments, in particular those involving selective laser excitation are clearly required to better understand the contribution of the various phenomena: multiple site formation in the polycrystalline Ar and N_2 matrices, low-frequency perylene modes, and intermolecular modes of perylene–rare gas and perylene–N_2 pseudocomplexes. Such experiments are now in the planning stage and will be reported separately.

[1] (a) A. Léger and J. L. Puget, Astron. Astrophys. **137**, L5 (1984); (b) L. J. Allamandola, A. G. G. M. Tielens, and J. R. Barker, Astrophys. J. Lett. **290**, L25 (1985).
[2] (a) G. P. Van der Zwet and L. J. Allamandola, Astron. Astrophys. **146**, 76 (1985); (b) A. Léger and L. B. d'Hendecourt, *ibid.* **146**, 81 (1985); (c) M. K. Crawford, A. G. G. M. Tielens, and L. J. Allamandola, Astrophys. J. Lett. **293**, L45 (1985); (d) F. Salama, E. L. O. Bakes, L. J. Allamandola, and A. G. G. M. Tielens, Astrophys. J. **458**, 621 (1996).
[3] (a) G. H. Herbig, Annu. Rev. Astron. Astrophys. **33**, 19 (1995); (b) P. Jenniskens and F. X. Désert, Astron. Astrophys., Suppl. Ser. **106**, 39 (1994); (c) G. H. Herbig and K. D. Leka, Astrophys. J. **382**, 193 (1991); (d) C. Joblin, J. P. Maillard, L. d'Hendecourt, and A. Léger, Nature (London) **346**, 729 (1990).
[4] (a) F. Salama and L. J. Allamandola, J. Chem. Phys. **94**, 6964 (1991); (b) F. Salama and L. J. Allamandola, Astrophys. J. **395**, 301 (1992).
[5] F. Salama and L. J. Allamandola, Nature (London) **358**, 42 (1992).
[6] A. Léger, L. d'Hendecourt, and D. Défourneau, Astron. Astrophys. **293**, L53 (1995).
[7] (a) J. Fulara, D. Lessen, P. Freivogel, and J. P. Maier, Nature (London) **366**, 439 (1993); (b) M. Tulej, D. A. Kirkwood, M. Pachkov, and J. P. Maier, Astrophys. J. Lett. **506**, L69 (1998); (c) B. H. Foing, and P. Ehrenfreund, Nature (London) **369**, 296 (1994).
[8] *The Diffuse Interstellar Bands*, edited by A. G. G. M. Tielens and T. P. Snow (Kluwer, Dordrecht, 1995).
[9] S. M. Scarrott, S. Watkin, J. R. Miles, and P. J. Sarre, Mon. Not. R. Astron. Soc. **255**, 11P (1992).
[10] G. D. Schmidt, M. Cohen, and B. Margon, Astrophys. J. Lett. **239**, L133 (1980).
[11] N. K. Rao and D. L. Lambert, Mon. Not. R. Astron. Soc. **263**, L27 (1993).
[12] (a) O. Braltbart, E. Castellucci, G. Dujardin, and S. Leach, J. Phys. Chem. **87**, 4799 (1983); (b) V. E. Bondybey and T. A. Miller, in *Molecular Ions: Spectroscopy, Structure and Chemistry*, edited by T. A. Miller and V. E. Bondybey (North-Holland, New York, 1983), p. 125; (c) C. J. M. Brugman, R. P. H. Rettschnick, and G. J. Hoytink, Chem. Phys. Lett. **8**, 263 (1971).
[13] C. Joblin, F. Salama, and L. Allamandola, J. Chem. Phys. **102**, 9743 (1995).
[14] F. Salama, C. Joblin, and L. J. Allamandola, J. Chem. Phys. **101**, 10252 (1994).
[15] (a) Y. Tanizaki, T. Yoshinaga, and H. Hiratsuka, Spectrochim. Acta A **34**, 205 (1978); (b) M. S. Gudipati, J. Phys. Chem. **98**, 9750 (1994).
[16] B. F. MacDonald, J. L. Hammons, R. R. Gore, J. R. Maple, and E. L. Wehry, Appl. Spectrosc. **42**, 1079 (1988).
[17] J. Szczepanski, C. Chapo, and M. Vala, Chem. Phys. Lett. **205**, 434 (1993).
[18] T. Tamm and P. Saari, Chem. Phys. **40**, 311 (1979).
[19] (a) C. Bouzou, C. Jouvet, J. B. Leblond, Ph. Millie, A. Tramer, and M. Sulkes, Chem. Phys. Lett. **97**, 161 (1983); (b) B. Fourmann, C. Jouvet, A. Tramer, J. M. Le Bars, and Ph. Millie, Chem. Phys. **92**, 25 (1985); (c) S. A. Schwartz and M. R. Topp, *ibid.* **86**, 245 (1984).
[20] (a) J. B. Birks, in *Photophysics of Aromatic Molecules* (Wiley, London, 1970), p. 122; (b) N. I. Nijegorodov and W. S. Downey, J. Phys. Chem. **98**, 5639 (1994); (c) W. Siebrand, J. Chem. Phys. **47**, 2411 (1967).
[21] M. Sonnenschein, A. Amirav, and J. Jortner, J. Phys. Chem. **88**, 4214 (1984).
[22] S. J. Cyvin, B. N. Cyvin, and P. Klaeboe, Spectrosc. Lett. **16**, 239 (1983).
[23] F. Fillaux, Chem. Phys. Lett. **114**, 384 (1985).
[24] H. J. Jodl, in *Chemistry and Physics of Matrix-Isolated Species*, edited by L. Andrews and M. Moskovits (Elsevier, Amsterdam, 1989), pp. 343–415.
[25] (a) M. M. Doxtader, I. M. Gulis, S. A. Schwartz, and M. R. Topp, Chem. Phys. Lett. **112**, 483 (1984); (b) M. M. Doxtader and M. R. Topp, J. Phys. Chem. **89**, 4291 (1985); (c) S. A. Wittmeyer and M. R. Topp, *ibid.* **95**, 4627 (1991); (d) D. Bahatt, A. Heidenreich, N. Ben-Horin, U. Even, and J. Jortner, J. Chem. Phys. **100**, 6290 (1994).